

EVALUATION OF RADIOTHERAPY BEAMS ATTENUATION AND SCATTERING CAUSED BY A PRINTED PHANTOM FILLED WITH AN ORGANIC SOLUTION USED IN NANOPARTICLE SYNTHESIS

Eduardo L. Corrêa*, Brianna Bosch-Santos, Glauco R. Veneziani, Vitor Vivolo, Artur W. Carbonari and Maria da Penha A. Potiens

Instituto de Pesquisas Energéticas e Nucleares (IPEN / CNEN - SP)
Av. Professor Lineu Prestes 2242
05508-000 São Paulo, SP, Brazil
*educorrea1905@gmail.com

ABSTRACT

In the past years nanotechnology has been distinguishing as a quick growing field, with many medical applications including drug delivery and medical images. For medical procedures gold nanoparticles (AuNPs) have been widely studied. The characteristics that make this material a good option to improve radiosensitivity in a specific tissue are their stability in a biological ambient and affinity to polyethylene glycol, which reduces its toxicity in mammals. A good method to produce AuNPs for medical applications is thermal decomposition, which is known for providing homogenous nanostructures and narrow size distribution. This production process consists in mixing gold acetate in an organic solution containing diphenyl ether, oleylamine, oleic acid and 1,2 octanediol, which is kept in a temperature of 300 °C for about two hours. After cooled the mixture must be centrifuged and washed in order to obtain the nanostructured grains. In this study a behavior comparison between water and the organic solution was made. The goal is to verify the viability of using this solution, instead of water, with a 3D printed phantom, as a dosimetric reference, since the removal process of nanoparticles from this solution to take them to water may cause a huge material loss. The comparison procedure was made in an industrial X-ray system operating in a voltage range from 10 kV to 50 kV. The results presented a variation up to 42.2 % between water and the organic solution radiation attenuation and up to 30 % for radiation scattering.

1. INTRODUCTION

In the past years nanotechnology has been distinguishing as a quick growing field, with many applications in science and technology including information storage[1], drug delivery [2-4], medical images [5,6] and food additive[6].

Furthermore, nanotechnology and molecular biology integration provides a huge potential for medical applications, in diagnostic and therapy procedures, such as biomarkers and biological sensors, besides tumors detection and treatment.[3-7]

For these procedures gold nanoparticles (AuNPs) have been widely studied, including their behavior when irradiated by X and/or gamma ray[4,8-10]. AuNPs present some characteristics which make them a nice option to improve radiosensitivity in a tissue. They are very stable in a biological, and also have affinity to polyethylene glycol, which reduces its toxicity in mammals. [11,12]

Thermal decomposition is a good method to produce nanoparticles for medical applications, providing homogenous nanostructures and narrow size distribution. It is considered one of the best methods used in the nanoparticles synthesis due to the high quality of the produced materials. [13]

This method consists in mixing gold acetate in an organic solution containing diphenyl ether, oleylamine, oleic acid and 1,2 octanediol, which is heated to 300 °C for two hours, in a three-neck round bottom flask, using a heating mantle. The mixture, after cooled, must be centrifuged and washed in order to obtain the nanostructured grains. [14]

In this study a behavior comparison between water and the organic solution was made. The goal was to verify the viability of using this solution, instead of water, with a 3D printed phantom, as a dosimetric reference, since the removal process of nanoparticles from this solution to take them to water may cause a huge material loss.

The 3D printed phantom was developed and is being studied as a cheaper and an easier-handle substitute for PMMA (polymethylmethacrylate), which is widely used in dosimetric studies.

2. MATERIALS AND METHODOLOGY

2.1 Materials

The phantom was designed using SolidWorks® software and made in an UP 3D printer, plus 2 model (Fig. 1).

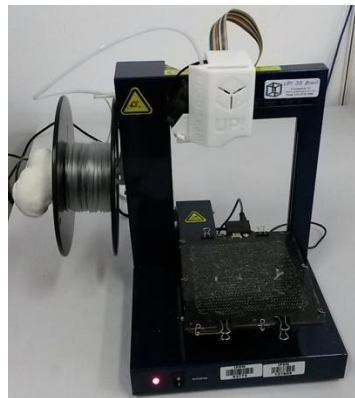


Figure 1: UP 3D printer, plus 2 model.

The first prototype was printed using ABS (Acrylonitrile Butadiene Styrene), which presents a density from 1060 kg/m³ to 1080 kg/m³ [15], and the second one was printed using PLA (Polylactic Acid), which density varies from 1210 kg/m³ to 1430 kg/m³ [16]. These materials are the cheapest and the most commonly used in this kind of 3D printer.

The X-ray beam was produced by an industrial X-ray system Pantak/Seifert, ISOVOLT 160 HS presented in Fig. 2, which has five series of reference radiation qualities established (mammography, diagnostic radiology, radiation protection, tomography and radiotherapy)[17-20]. This system can reach voltage up to 150 kV.



Figure 2: Industrial X-ray system Pantak/Seifert.

This study was made using the low-energy radiotherapy reference beams. Their main characteristics are presented in Table 1. Tube current of 10 mA was used.

Table 1: Low-energy radiotherapy radiation qualities main characteristics. Tube current of 10 mA was used.

Radiation quality	Tube Voltage (kV)	Half-value layer (mmAl)	Additional filtration (mmAl)	Air-kerma rate (mGy/s)
T-10	10	0.04	---	3.130
T-25	25	0.28	0.4	2.462
T-30	30	0.19	0.2	9.638
T-50 (a)	50	2.41	4	0.821
T-50 (b)	50	1.08	1	4.027

For attenuated beam measurement a parallel-plate PTW ionization chamber, 23344 model, volume of 0.20 cm³, which is highly recommended for surface low-energy radiotherapy beams measurements, was used (Fig. 3). This chamber was connected to a PTW electrometer, Unidos E model.



Figure 3: PTW ionization chamber, 23344 model, used in low-energy radiotherapy beams measurements.

For scattered radiation measurement a Radcal ionization chamber, RC180 model, volume of 180 cm³, connected to a Keithley electrometer, 6517A model, was used (Fig. 4). This chamber presents a good response both in diagnostic radiology and radiation protection beams measurements.



Figure 4: Radcal RC180 ionization chamber which can be used in both diagnostic radiology and radiation protection measurements.

In order to verify the radiation beam stability a PTW monitoring chamber, 34014 model, connected to a PTW electrometer, Unidos E model, was used.

2.2. Methodology

The tests were carried out positioning the printed phantom at 35 cm from the X-ray tube anode. The parallel plate PTW ionization chamber was placed 50 cm away from focal spot (reference distance) and Radcal chamber about 5 cm next to the phantom, as shown in Fig.5.

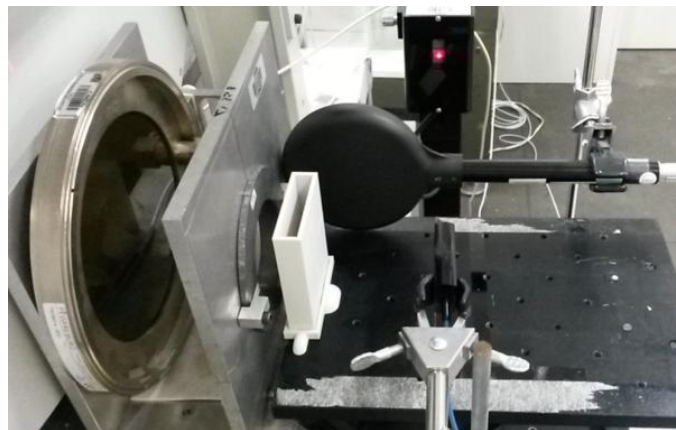


Figure 5: Experimental set up. The parallel plate PTW ionization chamber was placed to measure attenuated beam and the RC-180 chamber to measure the scattered radiation.

A set of ten measurements, 30 seconds each, was taken for each radiation qualities series, in four different conditions: no phantom; phantom fulfilled with 75 mL of water; with about 75 mL of the organic solution (a mix containing 60 mL of diphenyl ether, 6 mL of oleylamine, 6 mL of oleic acid and 4500 mg of 1,2 octanediol) and empty.

3. RESULTS AND DISCUSSION

3.1 Printed phantom development

Initially the phantom was printed with ABS material, but this material reacted with the organic solution, making it impossible to be used in this application. A test was performed with PLA, and since no reaction was observed a new phantom was printed (Fig. 6). The dimensions are 75 mm x 85 mm x 19 mm (width x height x depth). Wall thickness is 3 mm.

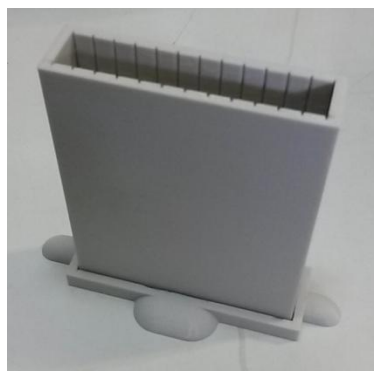


Figure 6: PLA printed phantom. Its dimensions are 75 mm x 85 mm x 19 mm (width x height x depth). Wall thickness is 3 mm.

3.2 Attenuation and scattering measurements

In Table 2 are shown a comparison between the charges collected by ionization chambers in measurements with and without the phantom presence.

Table 2: Comparison between both ionization chambers with and without the printed phantom presence

Radiation quality	Measurements without the phantom (nC)		Measurements with empty phantom (nC)	
	PTW 0709	Radcal RC-180	PTW 0709	Radcal RC-180
T-25	0.985 ± 0.030	0.498 ± 0.007	0.394 ± 0.012	1.168 ± 0.001
T-30	3.117 ± 0.047	1.165 ± 0.001	0.921 ± 0.001	2.743 ± 0.003
T-50(a)	0.300 ± 0.008	0.450 ± 0.001	0.253 ± 0.006	1.313 ± 0.001
T-50(b)	1.430 ± 0.021	1.417 ± 0.001	1.015 ± 0.001	4.263 ± 0.004

As expected when the printed phantom was placed in the radiation field it increased scattered radiation and decreased charges collected by PTW ionization chamber, a similar behavior was observed when compared to a PMMA phantom. The T-10 radiation quality could not be used because the printed phantom attenuated the most photons, causing a huge instability in ionization chambers measurements.

In Fig. 7 and Fig. 8 are shown, respectively, the variations in attenuation and scattering measurements obtained when the printed phantom was fulfilled first with water and then with the organic solution. The best fit for each situation was also presented. The variation presented in both cases is the result obtained when the phantom is fulfilled with water divided by the one when it is fulfilled with the organic solution. The uncertainties are around 5 %.

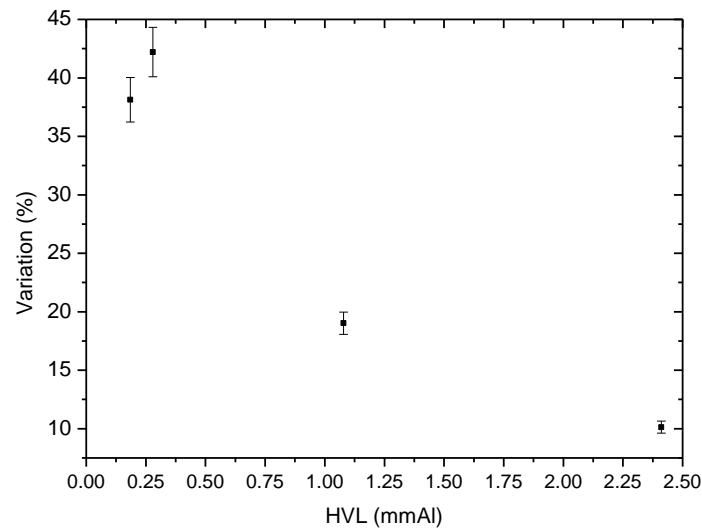


Figure 7: Comparison of radiation beam attenuation in both situations (variation between the phantom fulfilled with water and with the organic solution).

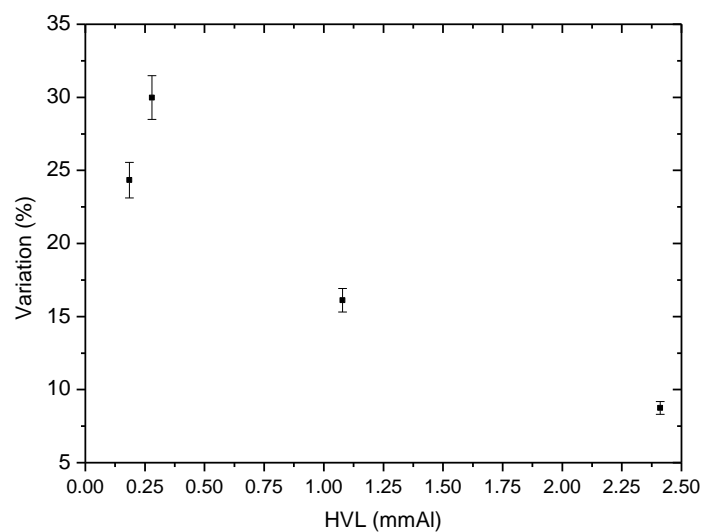


Figure 8: Comparison of radiation beam scattering in both situations (variation between the phantom fulfilled with water and with the organic solution).

The results have shown that, in both cases, the variation decreases as the energy increases. The major uncertainties are presented in the lower-energy qualities, as expected, since beams with so low energy are easily disturbed by any attenuator. Variations of up to 42.2 % (attenuation) and 30 % (radiation scattering) were observed.

Another interesting point is that water attenuated more than the organic solution, and produced less scattered radiation, which means that more amount of energy was deposited into this material. This result may indicate that dose enhancement caused by nanoparticles in the organic solution would be much more evident than in water.

Although it was not possible to make adjust in both comparisons, what causes difficulty to make measurements at intermediate energies (e.g. 40 kV), further tests will be made with same radiation qualities as those presented in this study. As long as the variations are well known the application of correction factors will be sufficient.

3. CONCLUSIONS

The printed phantom proved to be a cheaper and easier-handle alternative for PMMA, and 3D printer was able to produce an object that could store liquid materials. The attenuation and radiation scattering caused by this material to the radiation beam were measured.

Variations of up to 42.2 % (attenuation) and 30 % (radiation scattering) were observed. Water caused higher attenuation, and produced less scattered radiation than the organic solution, which means that more amount of energy was deposited into this material, what may indicate that dose enhancement caused by nanoparticles in the organic solution would be much more evident than in water.

Despite huge variations obtained in this study, further tests will be made in same conditions as those presented in this paper. Application of correction factors will be sufficient to overcome this problem.

ACKNOWLEDGMENTS

Authors acknowledge to CNPq, FAPESP and INCT, for partial financial support, to Prof. Leticia L. C. Rodrigues, for providing the 3D printer, and to Prof. Fernando B. Effenberger, for the help in the organic solution production.

REFERENCES

1. L. L. Vatta, R. D. Sanderson, K. R. Koch, "Magnetic nanoparticles: Properties applications," *Pure Appl. Chem.*, **v. 78**, n. 9, pp. 1793-1801 (2006).
2. Vinogradov, S. V., "Nanogels in the race for drug delivery," *Nanomedicine*, **v. 5**, n. 2, pp. 165–168 (2010).
3. O. V. Salata, "Applications of nanoparticles in biology and medicine," *Journal of Nanobiotechnology*, **v. 2**, n. 3 (2004).

4. E. Boisselier, D. Astruc, "Gold nanoparticles in nanomedicine: preparations, imaging, diagnostics, therapies and toxicity," *Chem. Soc. Rev.* **v. 38**, pp.1759–1782 (2009).
5. E. M. Pearce, J. B. Melanko, A. K. Salem, "Multifunctional Nanorods for Biomedical Applications," *Pharmaceutical Research*, **v. 24**, n. 12, p. 2335-2352 (2007).
6. M. A. Albrecht, C. W. Evans, C. L. Raston, "Green chemistry and the health implications of nanoparticles," *Green Chem.* **v. 8**, pp. 417–432 (2006).
7. D. Kwatra, A. Venugopal, S. Anant, "Nanoparticles in radiation therapy: a summary of various approaches to enhance radiosensitization in cancer," *Transl. Cancer Res.* **v. 2**, n. 4, pp. 330-342 (2013).
8. S. Cho, O. Vassiliev, S. Jang, S. Krishnan. "Modifications of megavoltage photon beams for gold nanoparticle-aided radiation therapy (GNRT): A Monte Carlo study," *Medical Physics.* **v. 33**, n. 6, pp. 2121-2121 (2006).
9. S. H. Cho, B. L. Jones, S. Krishnan, "The dosimetric feasibility of gold nanoparticle-aided radiation therapy (GNRT) via brachytherapy using low-energy gamma-/x-ray sources," *Phys. Med. Biol.* **v. 54**, pp. 4889–4905 (2009).
10. T. Marques, M. Schwarcke, C.E. Garrido, V. Zucolotto, O. Baffa, P. Nicolucci, "Gel Dosimetry Analysis of Gold Nanoparticle Application in Kilovoltage Radiation Therapy," *Journal of Physics: Conference Series - INTERNATIONAL CONFERENCE ON 3D DOSIMETRY*, Hilton Head, **v. 250**, n. 6, pp. 415-419 (2010).
11. E. Lechtman, N. Chattopadhyay, Z. Cai, S. Mashouf, R. Reilly, J. P. Pignol, "Implications on clinical scenario of gold nanoparticle radiosensitization in regards to 17 photon energy, nanoparticle size, concentration and location," *Physics in Medicine and Biology*, **v. 15**, pp. 4631-4647 (2011).
12. X. Liu, M. C. Lloyd, I. V. Fedorenko, P. Bapat, T. Zhukov, Q. Huo, "Enhanced imaging and accelerated photothermal analysis of A549 human lung cancer cells by gold nanospheres," *Nanomedicine*, **v. 5**, pp. 617-626 (2008).
13. A. H. Lu, E. L. Salabas, F. Schüth, "Magnetic nanoparticles: synthesis, protection, functionalization and application," *Angewandte Chemie-International Edition*, **v. 46**, n. 8, pp. 1222-1244 (2007).
14. Effenberger, F. B. *Nanomateriais magnéticos para aplicações em terapia e imagem*. Ph.D. Thesis - Instituto de Química, Universidade de São Paulo, São Paulo (2012).
15. "MATBASE: ABS General Purpose," <http://www.matbase.com/material-categories/natural-and-synthetic-polymers/commodity-polymers/material-properties-of-acrylonitrile-butadiene-styrene-general-purpose-gp-abs.html#properties> (2015).
16. "MATBASE: PLA monomere (Polylactic Acid)," <http://www.matbase.com/material-categories/natural-and-synthetic-polymers/agro-based-polymers/material-properties-of-polylactic-acid-monomere-pla-m.html#general> (2015).
17. E. L. CORRÊA, V. VIVOLO, M. P. A. POTIENS, "Quality control methodology and implementation of X-radiation standards beams, mammography level, following the standard IEC 61267," *Applied Radiation and Isotopes*, **v. online**, p. 1-4 (2012)
18. P. C. Franciscatto, *Caracterização das qualidades de radiação x seguindo as recomendações da norma iec 61267 no laboratório de calibração do IPEN*, Master Thesis - Instituto de Pesquisas Energéticas e Nucleares, Universidade de São Paulo, São Paulo (2009).
19. D. M. Dias, *Estabelecimento de um novo método de calibração de câmaras de ionização tipo lápis para dosimetria em feixes de tomografia computadorizada*, Master Thesis - Instituto de Pesquisas Energéticas e Nucleares, Universidade de São Paulo, São Paulo (2010).

20. A. C. M. BESSA, *Intercomparação de câmaras de ionização em feixes padrões de raios X, níveis radioterapia, radiodiagnóstico e radioproteção*, Master Thesis - Instituto de Pesquisas Energéticas e Nucleares, Universidade de São Paulo, São Paulo (2007).